



Data Mining II Project:

Analyzing Data Insights from the IMDb Platform

Authors:

Bruno Barbieri, Chiara Ferrara, Ankit Kumar Bhagat

Supervisors:

Prof. Riccardo Guidotti, Andrea Fedele

Academic Year 2024/2025

Computer Science Department

Contents

1	Data Understanding and Preparation	2
1.1	Feature Engineering	3
2	Outliers	4
2.1	Finding Baseline	4
2.2	Finding Threshold	4
2.3	Outlier Detection Conclusion	5
3	Imbalanced Learning	5
3.1	Oversampling	6
3.2	Undersampling	6
3.3	Decision Threshold	7
3.4	Imbalanced Learning Conclusion	7
4	Advanced Classification	7
4.1	Logistic Regression	8
4.2	Support Vector Machines	9
4.3	Ensemble methods	11
4.4	Neural Networks	13
4.5	Gradient Boosting Machines	15
4.6	Model Comparison	18
4.7	Explainable AI	18
4.7.1	titleType	18
4.7.2	averageRating	19
5	Advanced Regression	20
5.1	Random Forest Regression	20
5.2	Neural Network Regression	21
6	Time Series Analysis	21
6.1	Data Understanding	21
6.2	Motifs and Anomalies Discovery	22
6.3	Clustering	22
6.4	Classification	22
6.4.1	Recurrent Neural Network	22

Introduction

The goal of this report is to illustrate the characteristics of the given IMDb dataset, and to show key insights that can be obtained from it. The IMDb (**I**nternet **M**ovie **D**atabase) dataset is a comprehensive collection of information about films, TV shows, actors, crew, and more, compiled from IMDb's vast online database. Widely used in research and data science, this dataset includes various attributes such as movie titles, genres, release year, ratings, and reviews, among other details. The dataset is updated as of September 1, 2024.

1 Data Understanding and Preparation

The dataset contains 32 columns and 149531 rows of titles of different types. For each title, the dataset contains information regarding many different aspects. Table 1 lists the initial categorical features.

Feature	Description
<code>originalTitle</code>	Original title, in the original language (?)
<code>isAdult</code>	Whether or not the title is for adult
<code>canHaveEpisodes</code>	Whether the title can have episodes
<code>isRatable</code>	Whether the title can be rated by users
<code>titleType</code>	Type of the title (e.g., movie, tvseries)
<code>countryOfOrigin</code>	Countries where the title was primarily produced
<code>genres</code>	Genres associated with the title
<code>regions</code>	Regions for this version of the title
<code>soundMixes</code>	Technical specification of sound mixes
<code>worstRating</code> (ordinal)	Worst title rating
<code>bestRating</code> (ordinal)	Best title rating
<code>rating</code> (ordinal)	IMDB title rating class

Table 1: Initial categorical features of the IMDb dataset

Of the initial categorical attributes, the following were removed:

- `originalTitle`, as it did not provide particularly useful information;
- `isAdult`, as it was almost completely correlated with the *Adult* genre, so a logical OR operation was performed, and the genre only was kept;
- `canHaveEpisodes`, as it was completely correlated with the title type being *tvSeries* or *tvMiniSeries*;
- `isRatable`, as it was always true;
- `soundMixes`, as it required some domain knowledge to be understood, as well as having issues with the values it contained.
- `worstRating` and `bestRating`, as they were always 1 and 10, respectively;
- `rating`, as it was obtainable from the `averageRating` continuous attribute, through a simple discretization.

Table 2 lists the initial numerical features.

Feature	Description
startYear	Release year of the title (series start year for TV)
endYear	TV Series end year
runtimeMinutes	Primary runtime of the title, in minutes
numVotes	Number of votes the title has received
numRegions	Number of regions for this version of the title
totalImages	Total number of images for the title
totalVideos	Total number of videos for the title
totalCredits	Total number of credits for the title
criticReviewsTotal	Total number of critic reviews
awardWins	Number of awards the title won
awardNominations	Number of award nominations excluding wins
ratingCount	Total number of user ratings submitted
userReviewsTotal	Total number of user reviews
castNumber	Total number of cast individuals
CompaniesNumber	Total number of companies that worked for the title
averageRating	Weighted average of all user ratings
externalLinks	Total number of external links on IMDb page
quotesTotal	Total number of quotes on IMDb page
writerCredits	Total number of writer credits
directorCredits	Total number of director credits

Table 2: Initial numerical features of the IMDb dataset

Of the initial numerical attributes, the following were removed:

- **endYear**, as it had no values for non-Series titles, and having around 50% of missing values for *tvSeries* and *tvMiniSeries*;
- **numVotes**, as it had a very high correlation with **ratingCount**;

Figure ?? shows the skewness of some of the numerical features. It can be observed that many features exhibit a heavy right skew, with a long tail of high values.

Figure 1 shows the distribution of the **averageRating** attribute.

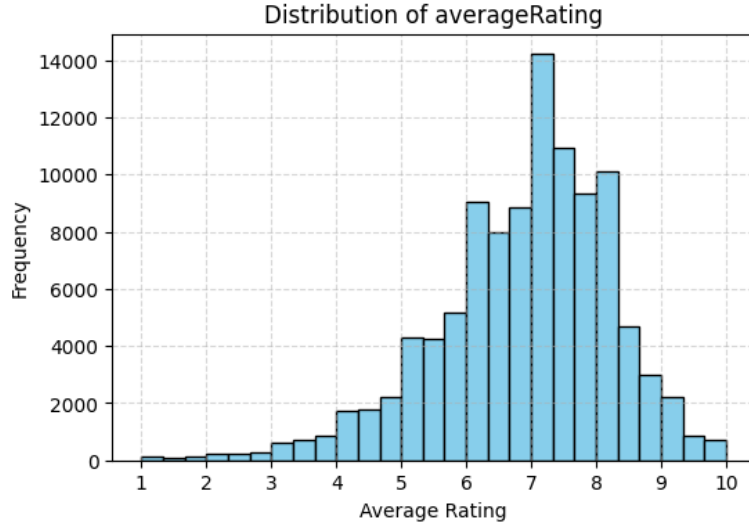


Figure 1: Distribution of the **averageRating** attribute

The distribution is Normal-like, with a peak around 7. This graph is particularly important because of the centrality of the feature in the classification and regression tasks.

1.1 Feature Engineering

- **totalImages**, **totalVideos** and **quotesTotal**, were merged through a simple sum operation into a single feature (**totalMedia**) because of their similar semantic meaning, as well as heavy right skewness;

- `awardWins` and `awardNominations`, were merged with the same procedure as above into `totalNominations`, since they represented the same concept;
- `userReviewsTotal` and `criticReviewsTotal`, were merged with the same procedure as above into `reviewsTotal`, since they represented the same concept;
- `regions` and `countryOfOrigin`, were merged through a simple union operation. The resulting feature was then represented through frequency encoding on the entire list, as well as counts of the number of countries from each continent. This resulted in eight new features (six continents, one for unknown country codes, and the last for the frequency encoding);
- `genre`, it was observed that each record contained up to three genres, listed in alphabetical order—indicating that the order did not convey any semantic information about the title. To represent this information, three separate features were created, each corresponding to one of the genres. These features were encoded using frequency encoding, sorted in descending order of frequency across the dataset. A value of 0 was used to indicate missing genres—either when no genres were present or to fill the remaining slots when fewer than three were available;
- `titleType`, was one-hot encoded, as it was a nominal categorical feature with no intrinsic order;
- `deltaCredits`, was created as the difference between `totalCredits` and the sum of `castNumber`, `writerCredits` and `directorCredits`. This feature aimed to capture the number of other types of credits (such as producers, editors, etc.) associated with a title, which could be relevant for understanding its production scale and complexity;
- `runtimeMinutes`, had a very high number of missing values approx 27%. Since the feature had high relevance in the domain, it was imputed with the interquartile range, separately for each title type. For advanced classification, in order to avoid any correlation with the target variable, we imputed the feature with random integers within the global interquartile range.

2 Outliers

2.1 Finding Baseline

In this outlier analysis section, our primary objective was to identify the top outliers in the dataset using three well-established methods- **Local Outlier Factor**, **Isolation Forest**, and **Angle-Based Outlier Detection**. To establish a baseline for model performance, we initially employed two supervised learning algorithms- **Decision Tree** and **K-Nearest Neighbors**. To enhance the alignment between the later module tasks we defined a categorical target variable, `rating_bin`, by dividing the continuous `averageRating` into six distinct classes. The classes were defined as follows:

$$0 = [0-5); 1 = [5-6); 2 = [6-7); 3 = [7-8); 4 = [8-9); \text{ and } 5 = [9-10]$$

The value count for each class was 12856, 19576, 37032, 49164, 25414, and 5489 respectively.

We then performed a grid search with cross-validation (`GridSearchCV`) on both models to identify the best hyperparameters. Since our dataset was large, we conducted the grid search on a 10% stratified sample to optimize computational efficiency. For K-NN, the optimal parameters were-

$$\text{metric} = \text{'manhattan'}, \text{n_neighbors} = 122, \text{weights} = \text{'distance'}$$

However, to strike a balance between accuracy and computational efficiency, we restricted our model to use 50 `n_neighbors`. For Decision Tree, the optimal parameters were-

$$\text{criterion} = \text{'gini'}, \text{max_depth} = 10, \text{min_samples_leaf} = 4, \text{min_samples_split} = 10, \text{splitter} = \text{'random'}$$

We trained both models on the entire training dataset and evaluated their performance on the test set. We split our training dataset into training (80%) and validation (20%) sets. We computed the baseline accuracy without removing any outliers, which was 36% for K-NN and 32% for Decision Tree.

2.2 Finding Threshold

Next, we applied the three outlier detection methods to identify and remove outliers from the training dataset. We experimented with different contamination levels (0.01, 0.05, 0.1) to determine the optimal proportion of outliers to remove. After removing the identified outliers, we retrained both models on the cleaned training dataset and evaluated their performance on the test set. We observed that removing outliers generally improved

		LOF	IF	ABOD
1%	KNN	42	42	41
	DT	39	39	40
5%	KNN	42	42	41
	DT	39	39	40
10%	KNN	43	42	41
	DT	40	39	40

Table 3: Accuracy at different threshold

model accuracy, but different contamination levels had no significant impact on the results as shown in table 3. Only the results from LOF with a contamination level of 0.1 showed an improvement of 1%. Therefore, we fixed the contamination level at 10% for all three methods to maintain consistency. Subsequently, we combined the results of the three methods by aggregating the outlier score and removed those rows that were flagged as outliers by at least **two out of the three methods**, which accounted for approximately 3% of the dataset.

2.3 Outlier Detection Conclusion

In conclusion, our anomaly detection task revealed a consistent trend: both models KNN and DT performed better than the baseline after the removal of outliers. This outcome sets the foundation for our subsequent focus on model explainability in the later sections.

From the T-SNE visualization, we observed that LOF predominantly identified outliers at the edges of the data distribution 2a, whereas IF detected them primarily within a clustered region 2b. ABOD, on the other hand, captured outliers both at the edges and within dense clusters 2c. This variation can be explained by the fundamental differences between the algorithms: LOF emphasizes anomalies in low-density regions, while IF isolates points distant from the main distribution. ABOD, which evaluates outliers based on the angular relationships of points, reflects a hybrid behavior by marking anomalies in both sparse and dense regions. Importantly, since the dataset is dominated by a single high-density region, most points lack anomalous neighbors, explaining why ABOD highlighted relatively fewer strong anomalies. To ensure computational efficiency, we implemented the 'fast' version of ABOD, which approximates angle-based detection using a specified number of neighbors rather than exhaustively computing angles across all data points.

Overall, as we can see from table 3 the removal of outliers with different threshold led to only marginal gains in predictive performance. However, the differences in detection patterns across methods provide valuable insights into the structure and density of the data distribution, reinforcing the importance of combining multiple approaches for a more comprehensive anomaly detection strategy. Therefore, we combined the results of all three methods to identify the common outliers.

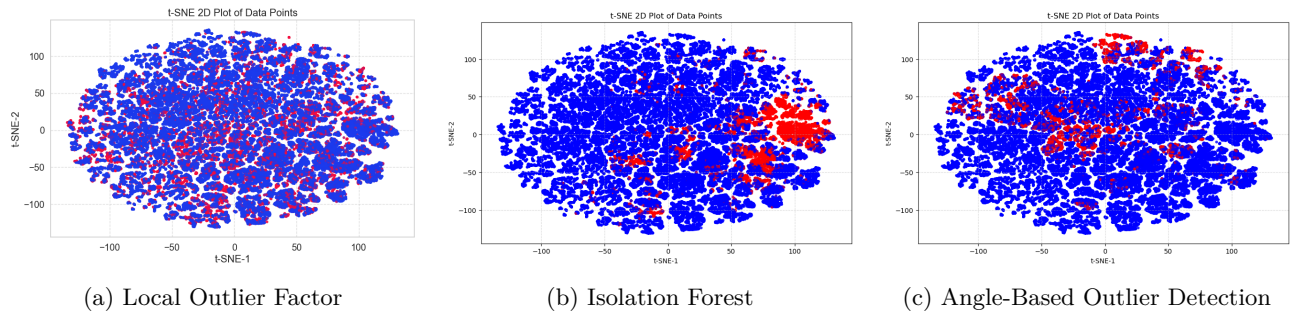


Figure 2: Comparison of T-SNE visualizations for different outlier detection methods.

3 Imbalanced Learning

We then proceeded with imbalance learning task, we used the same variable `averageRating` to categorize the data into three classes: low (0-4], medium (4-7], high (7-10]. The distribution of the classes is 4979, 67394, 72539 respectively, where the low class accounts for approx 3.5% of the dataset, which is highly imbalanced. We then applied Decision Tree classifier to the initial dataset and achieved 63% accuracy. Then we performed `RandomSearchCV` to tune the hyperparameters of the Decision Tree Classifier and achieved 67% accuracy. The best parameter were

Model Name	Accuracy	True Positives	Recall
Initial DT	63	200	0.20
HyperParameter Tuned DT	67	95	0.09
SMOTE	62	449	0.44
ADASYN	62	439	0.43
Resample	53	576	0.56
ENN	68	346	0.21
AllKNN	66	469	0.30
RandomUnderSampler + ENN	43	1307	0.82
DBSCAN + K-Means	56	907	0.57

Table 4: Imbalanced Learning Model Performance on Low (0-4] class

```
random_state=42, criterion='gini', max_features=None, max_depth=None, min_samples_leaf=10,
min_samples_split=2, splitter = 'random'
```

Our focus was to improve the recall of the low class, so we plotted the confusion matrix to see the number of true positives. As we can see from the table 4 the number of true positives for the low class had increased with different imbalanced learning techniques. Finally, we applied different imbalance learning techniques to improve the performance of the model.

3.1 Oversampling

In the oversampling techniques, we applied **Synthetic Minority Oversampling Technique (SMOTE)**, and **Adaptive Synthetic Sampling (ADASYN)** to increase the size of the minority class. Despite the different methodologies, SMOTE and ADASYN, both approaches resulted in nearly identical performance 62% accuracy and recall around 0.44-0.43 for the low class respectively 4. This highlights that while the oversampling strategy can influence which minority samples are emphasized, it does not fundamentally change the class distribution dynamics and may even introduce synthetic noise, thereby limiting overall accuracy improvements. As in our dataset both methods allowed the model to achieve similar overall accuracy and recall, indicating that the choice between these two oversampling techniques may not significantly impact performance in this specific context. The key difference lies in the sample generation strategy: **SMOTE** treats all minority samples equally during interpolation, whereas **ADASYN** focuses more on difficult-to-learn samples by adaptively weighting them according to their density in the feature space.. However, the similarity in results suggests that the dataset characteristics were such that both oversampling strategies provided comparable benefit in improving the model’s sensitivity to minority classes.

3.2 Undersampling

In the undersampling techniques, we applied **resample**, **Edited EditedNearestNeighbours (ENN)**, **AllKNN**, combination of **RandomUnderSampler + ENN** and clustering based undersampling using **DBSCAN + K-Means**. The best performance was achieved by **RandomUnderSampler + ENN** with 43% accuracy and 0.82 recall for the low class. **DBSCAN** and **K-Means** achieved 56% accuracy and 0.57 recall for the low class. The results were varied and sometimes counterintuitive, making it challenging to derive a single optimal strategy. For instance, the simple **resample** method achieved an accuracy of 53% with a recall of 0.56, indicating a balanced compromise between correctly predicting the majority class and detecting minority class instances. In contrast, **ENN** prioritized cleaning noisy or borderline samples, resulting in higher overall accuracy of 68% but a significantly lower recall of 0.21, reflecting poor sensitivity to the minority class. Similarly, **AllKNN**, which removes samples misclassified by all nearest neighbors, yielded a moderate accuracy of 66% and a recall of 0.30, suggesting that while it reduces noise, it also inadvertently removes some informative minority samples. The combination of **RandomUnderSampler + ENN** achieved an extreme result, with a low accuracy of 43% but a very high recall of 0.82, demonstrating that aggressive removal of majority class instances can drastically improve detection of the minority class at the cost of overall predictive correctness. Finally, the clustering-based approach (**DBSCAN + K-Means**) using **DBSCAN + K-Means** produced an accuracy of 56% and a recall of 0.57, which is relatively balanced, highlighting that clustering can preserve the structure of the data while reducing the majority class. In a nutshell we can say that: simple random resampling treats all samples equally, ENN and AllKNN remove noisy or ambiguous majority samples based on neighborhood consistency, the combined **RandomUnderSampler + ENN** aggressively removes majority instances to favor recall, and clustering-based undersampling attempts to retain representative majority samples while reducing redundancy. Overall, these experiments highlight the inherent trade-off in undersampling strategies between detecting minority classes and maintaining high overall accuracy, emphasizing that the choice of method should be guided by the specific priorities of the task.

For instance, in credit card fraud detection, aggressively undersampling legitimate transactions may help the model catch more fraudulent cases (**higher recall**) but can also cause more false alarms among genuine transactions (lower overall accuracy). The choice of undersampling method should therefore depend on whether catching fraud or avoiding false alarms is more critical.

3.3 Decision Threshold

After experimenting with both increasing and decreasing the training samples, we focused on the decision tree algorithm and attempted to adjust its decision threshold and class weights in the hypertuned model. We assigned higher importance to the minority class, **low** class, using the weights obtained from the **balanced** parameter, which were

'high': 0.6659, 'low': 9.7015, 'medium': 0.7167.

So, in this way the model would penalize misclassifications of the **low** class more heavily during training. It was surprising to see that even experimenting with different values of weights and assigning very high weight to **low** class could not lead to an increase in accuracy. In an attempt to further increase the recall of the **low** class, we also experimented with adjusting the decision threshold to shift the cutoff point for predicting each class after training. We modified the decision threshold to extreme values such as [0.1, 0.9, 0.1], the model's accuracy showed only marginal changes in decimals and consistently struggled to surpass the baseline accuracy of 67%. This suggests that the limitation may not be due to the model parameters or algorithmic tuning alone, but rather is inherently linked to the characteristics of the data. Both methods share the goal of improving minority class detection, yet their similarity lies in the fact that they cannot generate additional information; they only reweigh or reassign predictions based on existing patterns. The lack of improvement indicates that the features may not provide sufficient discriminatory power to separate the classes effectively, or that the classes themselves are inherently overlapping in the feature space.

3.4 Imbalanced Learning Conclusion

In conclusion, we can say that in an attempt to strive for both high **accuracy** and high **recall**, we carried out a series of extensive experiments. While our initial **DecisionTree** model achieved a reasonable accuracy of 63%, the recall was extremely low (0.20), reflecting its bias towards the majority class. After hyperparameter tuning, the accuracy improved to 67% but recall dropped further to 0.09. This counter-intuitive outcome can be attributed to the fact that tuning optimized for accuracy rather than recall, causing the model to become even more conservative in predicting the minority class. Oversampling techniques such as **SMOTE** and **ADASYN** substantially increased recall (0.44 and 0.43, respectively) because they synthetically generated minority samples, allowing the classifier to better recognize underrepresented patterns. However, this came at the cost of accuracy (dropping to 62%), since synthetic data can blur class boundaries and make the classifier more prone to misclassifications in the majority class. Undersampling approaches such as **Resample** and **RandomUnderSampler** + **ENN** achieved very high recall (0.56 and 0.82, respectively), but their accuracy decreased sharply (to 53% and 43%). The reason is that by aggressively reducing the majority class, these methods forced the classifier to focus disproportionately on the minority class, which inflated recall but degraded its ability to generalize across the full distribution. To understand the trade-offs more we looked at feature importance and we found out that the feature **tvEpisode** emerged as the most significant contributor across multiple models, while other features such as **startYear**, **genre1**, **genre2**, **castNumber**, and **totalCredits** also played crucial roles. However, the relative importance of these features varied across different models, indicating that no single feature consistently dominated in all approaches. Thus we were satisfied with the results of **SMOTE** and **ADASYN** as they provided a good balance between accuracy and recall.

4 Advanced Classification

In this section, classification results are showcased for two target variables: **averageRating** (properly binned into 6 classes), and **titleType** (with 6 classes).

We then applied multiple classification models using the data as preprocessed previously (see Section ??). The first target variable is **titleType**, which includes six categories: *movie*, *short*, *tvEpisode*, *tvSeries*, *tvSpecial*, and *video*. The classes are not equally distributed, with *tvSpecial* and *video* being significantly under-represented compared to the others. Entries labeled as *videoGame* were removed from both the training and testing sets, as they were too few to be useful for classification. The remaining categories were merged into broader groups according to the following mapping: *movie* and *tvMovie* were grouped as *movie*, *short* and *tvShort* were grouped as *short*, *tvSeries* and *tvMiniSeries* were grouped as *tvSeries*, while *tvEpisode*, *tvSpecial* and *video* were left unchanged. All feature columns were standardized using a *StandardScaler*. In addition, the

variable `canHaveEpisodes` was removed prior to training, since it provides direct information about the target `titleType` and could therefore introduce data leakage.

4.1 Logistic Regression

For the classification of the `titleType` variable, the target was transformed into numerical labels using `LabelEncoder` and all numerical features were scaled with `StandardScaler` to ensure comparability across variables. Since the problem is multi-class, we chose to present the results using the *One-vs-Rest (OVR)* approach, which trains a binary classifier for each class. We also tested the *multinomial* strategy, but it was significantly slower and produced comparable results, so OVR was selected for efficiency.

To optimize the model, a hyperparameter search was performed using `RandomizedSearchCV` with `StratifiedKfold` (5 folds), ensuring that the class distribution was preserved in each fold. The solver was set to `saga`, and the parameters tested included the regularization term `C` (50 values logarithmically spaced between 10^{-3} and 10^2), `penalty` (12 and 11), and `class_weight` (None and balanced). The hyperparameter search was performed using `f1_macro` as the scoring metric to balance performance across all classes. The best parameters selected by the search were **`C = 2.95`**, **`penalty = 11`**, and **`class_weight = balanced`**.

For computational efficiency, the search was conducted on a 10% stratified sample of the dataset, which was approximately representative of the original class distribution. The final model was then refitted on the full dataset using the best parameters. Evaluation on the test set was carried out using the confusion matrix, classification report, and one-vs-rest ROC curves for each class. The main performance metrics are summarized in Table 5, and the corresponding ROC curves are shown in Figure 3.

Table 5: Classification report for `titleType`

Class	Precision	Recall	F1-score
tvEpisode	0.90	0.88	0.89
movie	0.92	0.65	0.76
short	0.74	0.87	0.80
tvSeries	0.50	0.35	0.41
video	0.21	0.47	0.29
tvSpecial	0.07	0.52	0.12
Accuracy		0.75	
Macro avg	0.56	0.62	0.54
Weighted avg	0.83	0.75	0.78

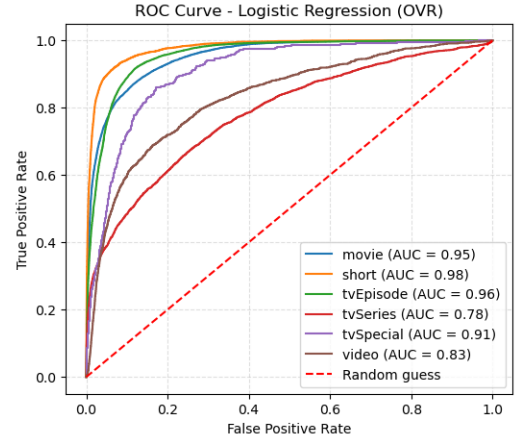


Figure 3: ROC Logistic Regression

From the results, we observe that the model achieves high performance for the `movie`, `short`, and `tvEpisode` classes, with F1-scores of 0.76, 0.80, and 0.89, respectively. The model performs less well on `tvSeries`, `tvSpecial`, and `video`, likely due to lower support in the dataset. Overall, the model reaches an accuracy of 0.75, a macro-average F1 of 0.54, and a weighted F1 of 0.78. These results highlight that while the model discriminates well among the more common classes, its performance is still limited for rarer classes. This pattern is also reflected in the ROC curves shown in Figure 3, where the model clearly separates the more frequent classes, while discrimination is more limited for the less common categories.

Furthermore, coefficient analysis highlighted the main drivers for each class. Globally, `totalNominations`, `numRegions`, and `runtimeMinutes` were most influential. For individual classes, for example, `movie` is positively influenced by `totalNominations` but negatively by `genre3`; `short` is positively influenced by `totalNominations` and negatively by `companiesNumber`; `tvEpisode` is positively influenced by `Europe` and negatively by `numRegions`. Building upon the approach described for `titleType`, we trained a Logistic Regression model for the multi-class `rating_class` variable. All numerical features were scaled and, in addition, the categorical variable `titleType` was included as a predictor and processed via *One-Hot Encoding*.

Hyperparameters were optimized using again `RandomizedSearchCV` with `StratifiedKfold` (5 folds), performed on a 10% stratified sample of the data for computational efficiency. The scoring metric was `f1_macro`, and the search explored the same set of parameters used for `titleType`. The optimal configuration was found to be: **`C = 0.08`**, **`penalty = 12`**, and **`class_weight = balanced`**.

The best parameters were then used to fit the model on the full dataset, and evaluation on the test set was carried out.

The results for the `rating_class` target are reported in Table 6 and Figure 4. Overall, the model shows limited predictive ability (**`accuracy = 0.27`**, **`macro F1 = 0.25`**), with marked variability across classes. The extreme

intervals, [1,5) and [9,10), are detected with relatively high recall (0.44 and 0.57), but their low precision yields modest F1-scores. In contrast, the central ranges, which dominate the distribution, prove more difficult to classify: [6,7) reaches only 0.13 in F1, while [7,8) performs better at 0.40.

Regarding ROC curves: discrimination is stronger for the extreme categories (AUCs of 0.75 and 0.76), whereas separability is weaker in the central intervals ([6,7): 0.60, [7,8): 0.64). This suggests that Logistic Regression tends to distinguishing the most polarized cases, while it struggles to capture subtle differences in the middle of the rating scale.

Table 6: Classification report for `rating_class`

Class	Precision	Recall	F1-score
[1, 5)	0.20	0.44	0.27
[5, 6)	0.26	0.32	0.29
[6, 7)	0.39	0.08	0.13
[7, 8)	0.48	0.34	0.40
[8, 9)	0.25	0.22	0.24
[9, 10)	0.09	0.57	0.16
Accuracy		0.27	
Macro avg	0.28	0.33	0.25
Weighted avg	0.35	0.27	0.27

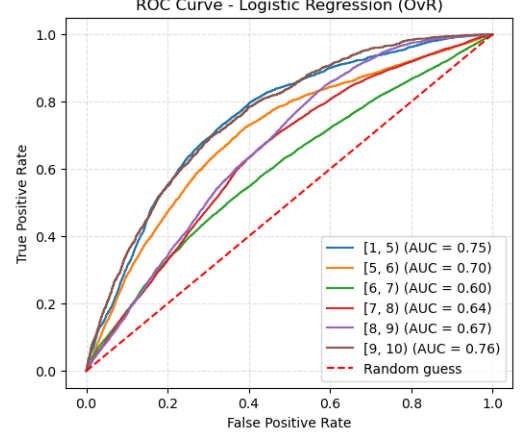


Figure 4: ROC curves for `rating_class` (OvR)

4.2 Support Vector Machines

We applied Support Vector Machines (SVM) to the `titleType` classification task. Both linear and non-linear kernels were explored in order to evaluate how decision boundary complexity influences predictive performance. The first experiment used a Linear SVM trained on the full dataset. A grid search with five-fold cross validation was carried out on the parameters $C \in \{0.01, 0.1, 1, 10, 100\}$ and $max_iter \in \{1000, 5000, 10000\}$. The optimal configuration, with $C = 100$ and $max_iter = 1000$, achieved a test accuracy of 0.81. While precision and recall were high for majority classes (*movie*, *short*, *tvEpisode*), the classifier failed on *tvSeries*, *tvSpecial*, and *video*, indicating that a linear decision boundary is insufficient for this problem.

Non-linear kernels were then evaluated. A grid search was first performed on a stratified 10% subset of the training set to efficiently explore a wide range of hyperparameters for each kernel, since a full search on the complete dataset would have been computationally prohibitive. All kernels were tested with C ranging from 0.01 to 100 and γ set to `scale` or `auto`. For the polynomial kernel, the degree was varied between 2 and 4 and `coef0` set to 0 or 1. For the sigmoid kernel, `coef0` was also explored at 0 and 1.

The best configuration for each kernel, reported in Table 7, was then retrained on the full dataset and evaluated on the test set. Both RBF and polynomial kernels reached approximately 0.90 test accuracy, substantially outperforming the linear baseline and sigmoid. The RBF kernel was selected as the reference non-linear model due to slightly more stable results and improved recall on the under-represented classes.

To address class imbalance, the RBF kernel was retrained with `class_weight=balanced`. This model reached a slightly lower overall accuracy of 0.84, but recall for *tvSpecial* and *video* improved, providing a more equitable classification across categories. The corresponding ROC curves (Figure 5b) show high separability for all classes, with AUC values of 0.99 for *movie*, *short*, and *tvEpisode*, and 0.95 for *tvSeries*, *tvSpecial*, and *video*, confirming that the balanced model achieves good discrimination for the minority categories too.

Then an analysis of the support vectors was conducted. In the unbalanced RBF, nearly all points of minority classes became support vectors, while in the balanced model the total number of support vectors increased but was more evenly distributed across classes, indicating a more complex but fairer decision function.

Table 7 summarizes the main results, including the parameters used for each kernel and the corresponding test performance.

Support Vector Machines were applied to the `averageRating` classification task using the same kernels and hyperparameter search strategies as for `titleType`. A Linear SVM achieved only 0.37 accuracy and a macro F1-score of 0.28, indicating that a linear decision boundary is inadequate.

Non-linear kernels were then explored. Both RBF and polynomial kernels reached similar test accuracy around 0.39, substantially outperforming the sigmoid kernel (0.28). Due to slightly more stable results and better handling of minority categories, the RBF kernel was selected as the reference model.

Table 7: Comparison of SVM models on the IMDb classification task.

Model	Best Params (main)	Test Accuracy	Macro F1-score
Linear SVM	$C = 100$, $max_iter = 1000$	0.81	0.45
RBF kernel	$C = 10$, $\gamma = scale$	0.90	0.64
Polynomial kernel	$C = 10$, $degree=3$, $\gamma = auto$	0.90	0.64
Sigmoid kernel	$C = 0.1$, $\gamma = auto$	0.65	0.36
RBF (balanced)	$C = 10$, $\gamma = scale$, balanced	0.84	0.65

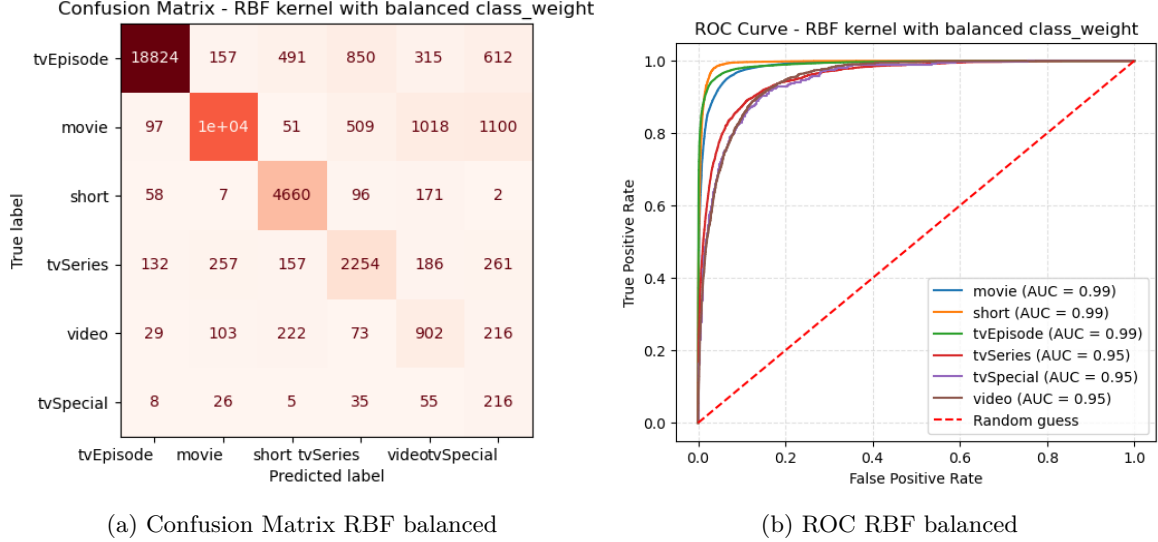


Figure 5: Confusion Matrix and ROC Curve for the SVM (kernel rbf and balanced class weight) on the titleType classification task.

To address class imbalance, the RBF model was retrained with `class_weight=balanced`. Overall accuracy decreased slightly to 0.29, but recall improved for the minority classes, particularly the extreme bins [1, 5) and [9, 10). The classification report shows that the model captures a high proportion of extreme instances (recall 0.55 for [1, 5) and 0.63 for [9, 10)), although precision is low (0.23 and 0.10, respectively), resulting in moderate F1-scores (0.33 and 0.18). Intermediate bins are predicted with higher precision but lower recall, reflecting the difficulty of separating densely populated central categories.

ROC curves confirm this pattern: AUC is highest for the extremes ([1, 5): 0.79, [9, 10): 0.80) and lower for intermediate bins ([6, 7): 0.61, [7, 8): 0.65), indicating that the model distinguishes extreme ratings better than the mid-range values.

Overall, non-linear kernels improve performance over linear SVM, but the ordinal nature of `averageRating` and the strong class imbalance continue to challenge accurate prediction across all bins.

4.3 Ensemble methods

Boosting and Random Forest models were trained on the classification tasks, while being optimized via Stratified Randomized Search with 5-fold cross-validation over a predefined hyperparameter space.

Table 8 shows the best hyperparameters found for Random Forest and AdaBoost on the **averageRating** task.

For Random Forest, a relatively high maximum depth as well as low values for minimum samples per split and leaf indicate that the individual trees are quite complex.

For AdaBoost, the base estimator is again characterized by high complexity. The learning rate is moderate, leading to reasonably fast learning.

Random Forest	
n_estimators	97
max_depth	19
min_samples_split	2
min_samples_leaf	6
max_features	0.91
criterion	gini
class_weight	None
AdaBoost	
n_estimators	67
learning_rate	0.45
estimator__max_depth	17
estimator__min_samples_split	7
estimator__min_samples_leaf	1

Table 8: Hyperparameters found for ensemble models.

The two models use a different number of estimators, with Random Forest employing a larger ensemble. This is likely due to the fact that Random Forest builds trees independently, while AdaBoost adds weak learners sequentially, focusing on correcting previous errors.

Another interesting aspect is the distribution of feature importances. Both models assign most of the importance to the same set of features:

- **ratingCount**
- **startYear**
- **runtimeMinutes**
- **deltaCredits**

Random Forest assigns about 50% of the total importance to these features, spreading it evenly among them. AdaBoost assigns about 75%, 41 of which is attributed to **ratingCount** and **startYear**.

Table 9 summarizes the classification report for both models. Although the performances of the two models are similar, Random Forest outperforms AdaBoost in all metrics but Macro-averaged Precision. The weighted averaged metrics, here not reported, also give the edge to Random Forest.

Model	Accuracy	Macro Precision	Macro Recall	Macro F1-score
Random Forest	0.45	0.47	0.35	0.37
AdaBoost	0.43	0.49	0.33	0.35

Table 9: Performances of the models on the **averageRating** classification task.

Performances of both models are limited, and the results show that the different classes are not well separated. This can be observed in Random Forest’s confusion matrix in figure 6a. The matrix also shows that many of the misclassifications occur within adjacent classes, which is expected given the ordinal nature of the target variable. In particular, a lot of confusion occurs between the most represented classes, [6,7), [7,8) and [8,9). This is likely due to the fact that these classes cover a wide variety of titles that perform similarly in terms of ratings. Additionally, as seen in graph 1, Many of the titles have ratings that fall close to the boundaries between these classes, making it more difficult for the model to distinguish between them.

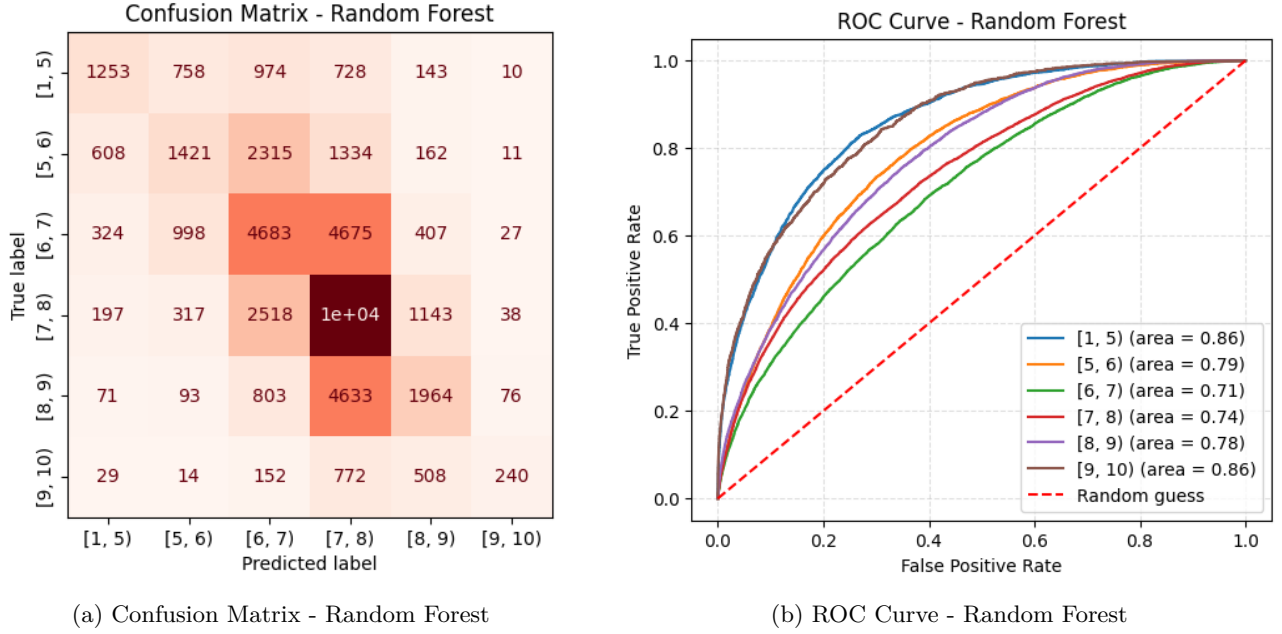


Figure 6: Confusion matrix and ROC Curve for Random Forest on the `averageRating` classification task.

Figure 6b shows the ROC curve for AdaBoost. AUCs are generally high, with the lowest ones being 0.70 and 0.72, although these correspond to the highest-represented classes. This suggests that the models are better at separating the extreme classes, while the more frequent intermediate ones are more difficult to distinguish.

Table 10 shows the best hyperparameter configurations found for Random Forest and AdaBoost on the `titleType` task.

For Random Forest, the trees are quite deep and complex, with low minimum samples per split and leaf.

For AdaBoost, the learning rate is very low, leading to slow, incremental learning. The base estimator is a decision tree with considerable depth and higher minimum samples per split and leaf than Random Forest’s trees, indicating that each weak learner is slightly less complex.

Again, the two models use a very different number of estimators, with Random Forest employing a much larger ensemble. For feature importances, both models assign over half of the importance to `runtimeMinutes`, indicating a high dependence on this feature for classification.

Random Forest	
<code>n_estimators</code>	42
<code>max_depth</code>	19
<code>min_samples_split</code>	4
<code>min_samples_leaf</code>	3
<code>max_features</code>	0.74
<code>criterion</code>	gini
<code>class_weight</code>	None
AdaBoost	
<code>n_estimators</code>	11
<code>learning_rate</code>	0.03
<code>estimator__max_depth</code>	14
<code>estimator__min_samples_split</code>	18
<code>estimator__min_samples_leaf</code>	10

Table 10: Hyperparameter search space for ensemble models.

Table 11 summarizes the classification report for both models.

Model	Accuracy	Macro Precision	Macro Recall	Macro F1-score
Random Forest	0.92	0.84	0.71	0.75
AdaBoost	0.92	0.81	0.70	0.73

Table 11: Performances of the models on the `titleType` classification task.

Figures 7a shows the confusion matrix for Random Forest. Consistently good performances can be observed across the most represented classes. `video` and `tvSpecial` are the classes that cause the most problems, since they are often misclassified as the more frequent classes. The class `movie` attracts most of these misclassifications, likely due to similar durations of the products in these categories. Likely due to the same reason, `video` is also often misclassified as `short`.

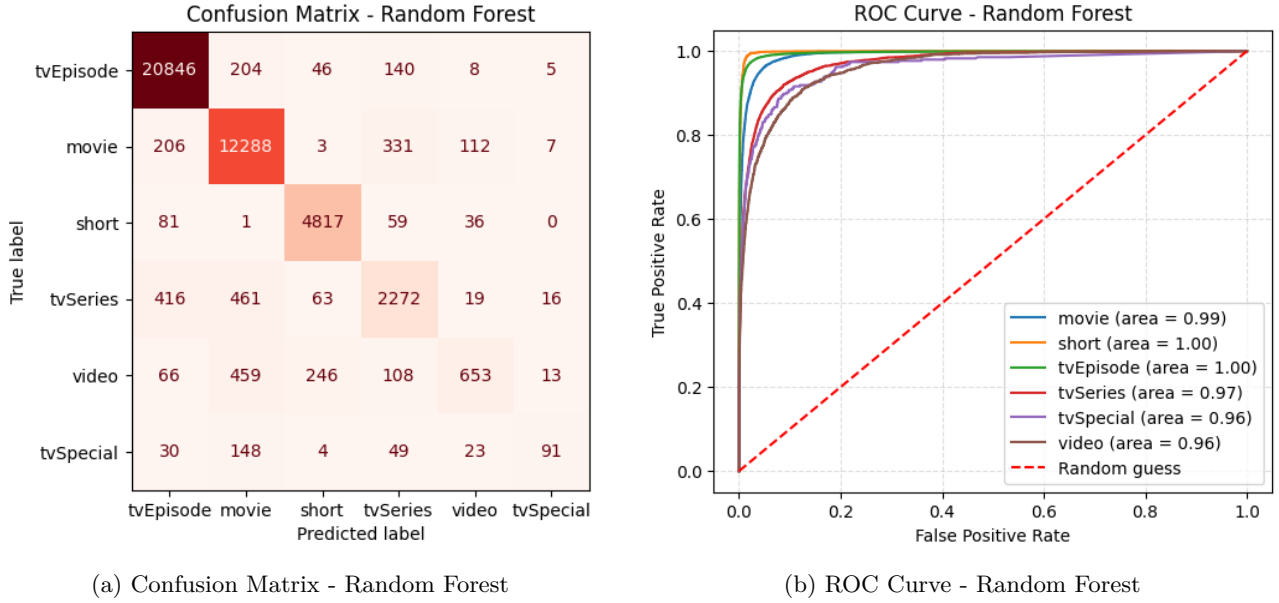


Figure 7: Confusion matrix and ROC Curve for Random Forest on the `titleType` classification task.

The ROC curve shows high AUCs for all classes, with the lowest ones being for the aforementioned less represented classes, both achieving 0.96. This indicates that the model is very good at maintaining a low false positive rate for these, while correctly identifying the more represented classes.

4.4 Neural Networks

For both classification tasks, a feedforward neural network was implemented.

For the `averageRating` task, the architecture consists of an input layer, six hidden layers with ReLU activation, forming a diamond shape (increasing and then decreasing number of neurons), a dropout layer (rate 0.2) to prevent overfitting, and an output layer with softmax activation for multi-class classification.

The model was compiled with the Adam optimizer, categorical cross-entropy loss, and accuracy as the evaluation metric. No early stopping was used, in order to observe the full training dynamics. Training was set to last for 500 epochs, with a batch size of 64 and a validation split of 20%.

Figures 8a and 8b show the training and validation loss and accuracy over epochs. The training loss shows a steady decrease, while the validation loss stops improving after around 100 to 150 epochs. A similar trend is observed in the accuracy plot, although the end of the the rise can be found after around 200 epochs. Neither graph shows particular signs of overfitting, but the stagnation of the validation metrics suggests that the model could benefit from further regularization. Experiments were made with different dropout rates and configurations, as well as different training batch sizes and learning rates, in an attempt to improve generalizaiton, but this remained the best configuration found.

	Precision	Recall	F1-score
Macro avg	0.39	0.29	0.29
Weighted avg	0.39	0.40	0.36
Accuracy	0.40		

Table 12: Classification performances for the neural network on the `averageRating` classification task.

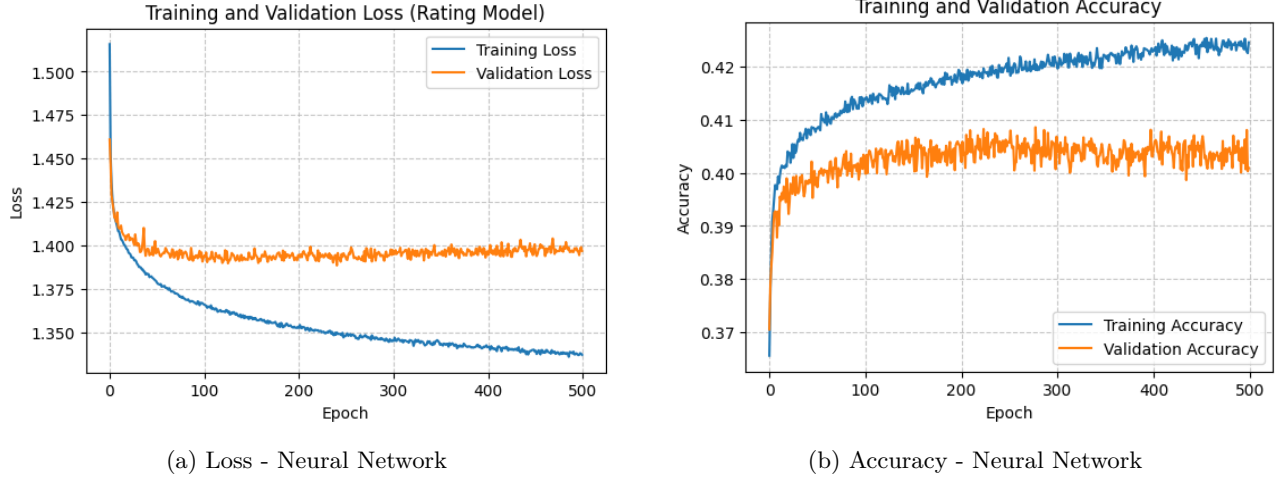


Figure 8: Training and validation loss and accuracy for the neural network on the `averageRating` classification task.

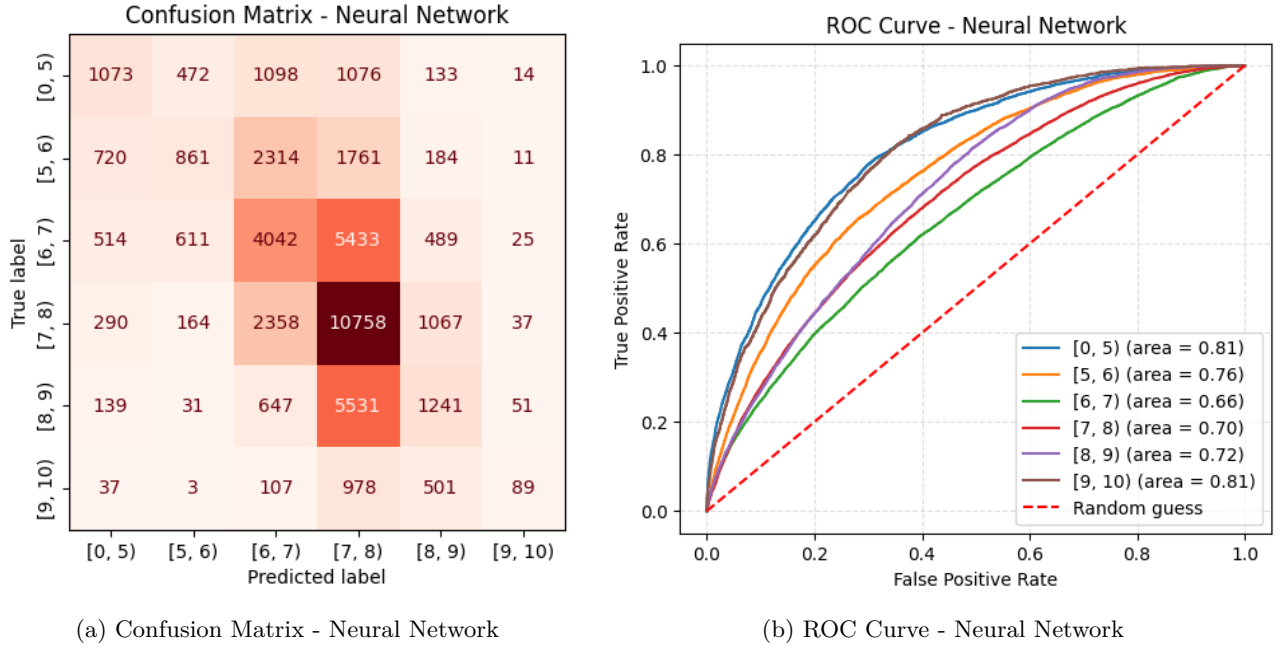
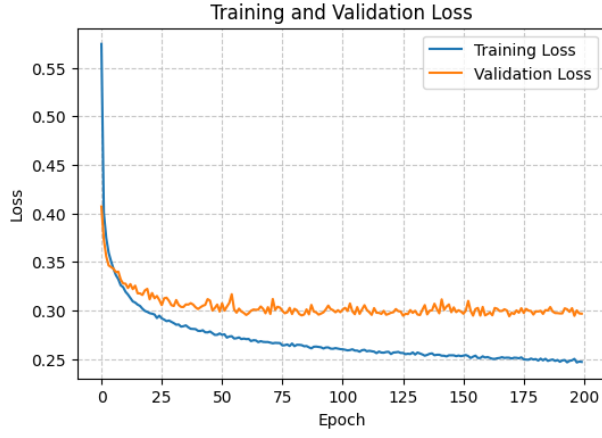
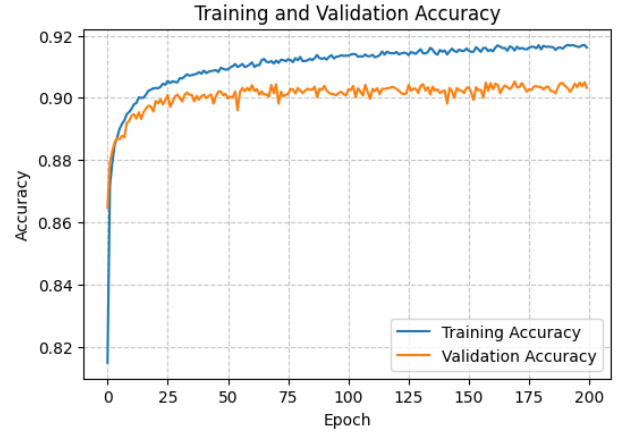


Figure 9: Confusion Matrix and ROC Curve for the Neural Network on the `averageRating` classification task.

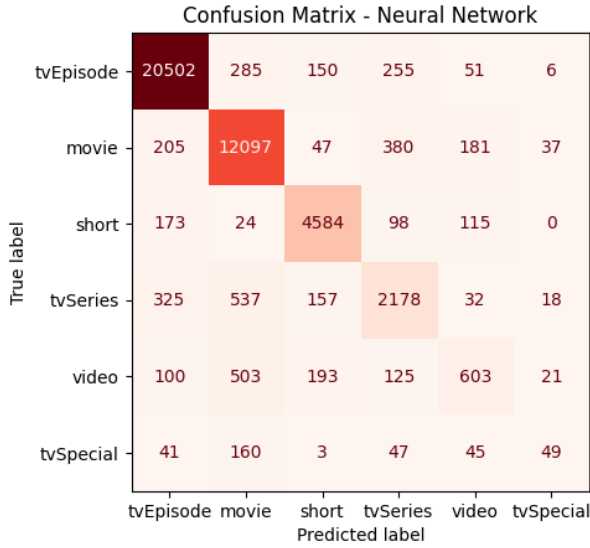


(a) Loss - Neural Network

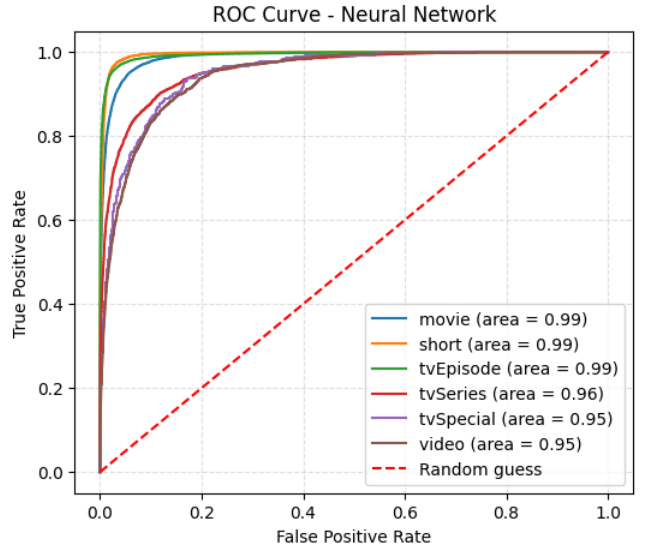


(b) Accuracy - Neural Network

Figure 10: Training and validation loss and accuracy for the neural network on the `titleType` classification task.



(a) Confusion Matrix - Neural Network



(b) ROC Curve - Neural Network

Figure 11: Confusion Matrix and ROC Curve for the Neural Network on the `titleType` classification task.

4.5 Gradient Boosting Machines

Next, we applied a **Gradient Boosting Machine (GBM)** to evaluate its ability to classify the `titleType` and `rating_bin` variable. GBM is an ensemble method that builds a series of decision trees sequentially, where each tree attempts to correct the errors of its predecessor. Unlike **Random Forest**, which builds trees independently and averages their predictions, GBM focuses on minimizing the loss function through gradient descent, making it highly adaptive to complex patterns in the data. The baseline accuracy to predict `titleType` was found out to be 0.94, while for `rating_bin` it was 0.40. For both tasks, we sampled the data to 10% of the training set to perform hyperparameter tuning, due to the high computational cost of training GBM models on large datasets. The hyperparameter tuning was performed using **RandomizedSearchCV** with 5-fold stratified cross-validation. Table 13 shows the best parameters found for the `titleType` and `rating_bin`.

titleType	
subsample	0.8
n_estimators	500
max_depth	6
min_samples_split	10
min_samples_leaf	1
max_features	None
learning_rate	0.1
rating_bin	
subsample	0.6
n_estimators	400
max_depth	5
min_samples_split	10
min_samples_leaf	2
max_features	sqrt
learning_rate	0.05

Table 13: Hyperparameter search space for GBM.

Table 14: Classification report for titleType

Class	Precision	Recall	F1-score
tvEpisode	0.94	0.97	0.96
movie	0.95	0.98	0.97
short	0.98	0.98	0.98
tvSeries	0.94	0.97	0.96
video	0.77	0.45	0.57
tvSpecial	0.79	0.55	0.65
Accuracy		0.96	
Macro avg	0.90	0.82	0.85
Weighted avg	0.96	0.96	0.96

Confusion Matrix - Gradient Boosting Machine							
True Label	tvEpisode	13684	136	24	57	8	2
	movie	149	8200	5	29	85	10
	short	30	1	2992	2	35	0
	tvSeries	30	17	0	1906	4	1
	video	43	258	118	21	567	17
	tvSpecial	15	68	1	16	20	99
		tvEpisode	movie	short	tvSeries	video	tvSpecial

Figure 12: Confusion Gradient Boosting Machine

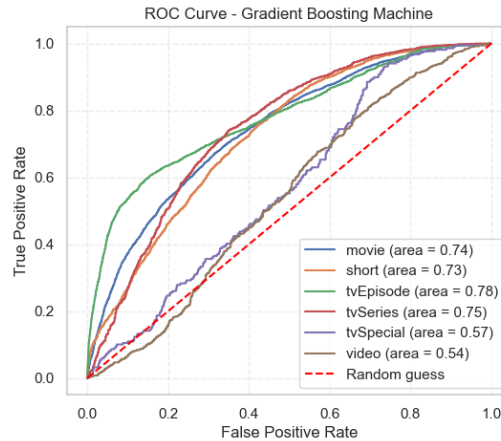


Figure 13: ROC Gradient Boosting Machine

From the table 14, we can see that GBM performs very well on the **titleType** task, achieving an accuracy of 0.96. The confusion matrix (Figure 12) shows that the model is able to correctly classify most of the classes, with only a few misclassifications recorded for the less represented classes **video** and **tvSpecial**. The ROC curves (Figure 13) also show high AUC values for all classes, indicating that the model is able to separate the classes well. The differences in ROC curve suggest that the model is more effective at distinguishing

structured and well-documented categories such as *tvEpisode*, *tvSeries*, and *movie*. To further investigate, we examined feature importance and found that `runtimeMinutes`, `numRegions`, and `directorCredits` were among the most influential features. Titles with longer runtimes and broader regional distribution were more likely to be classified as *movies* or *tvSeries*, while shorter or regionally limited titles tended to fall into categories like *short* or *video*. The number of director credits also served as a proxy for production quality and documentation, helping the model differentiate between professionally produced content and less formal formats. Interestingly, the *Europe* feature emerged as a strong predictor, possibly due to cultural or market-specific trends in title type distribution.

Table 15: Classification report for `titleType`

Class	Precision	Recall	F1-score
0	0.49	0.38	0.43
1	0.37	0.26	0.31
2	0.41	0.39	0.40
3	0.47	0.67	0.56
4	0.43	0.30	0.35
5	0.44	0.22	0.29
Accuracy		0.44	
Macro avg	0.44	0.37	0.39
Weighted avg	0.44	0.44	0.43

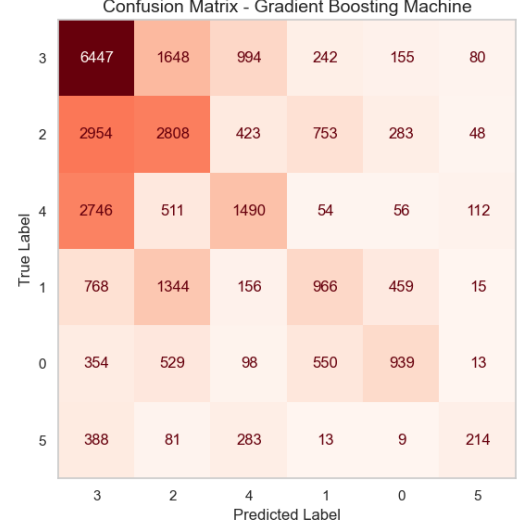


Figure 14: Confusion Matrix Gradient Boosting Machine

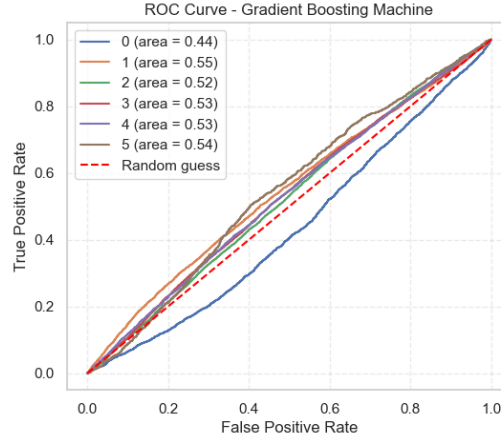


Figure 15: ROC Gradient Boosting Machine

From the table 15, it is evident that the Gradient Boosting Machine performs moderately on the `rating_bin` classification task, achieving an overall accuracy of 0.44. While this is less than 50%, considering that the task involves six classes, the model exceeds the baseline accuracy of $1/6$, indicating that it is capturing some underlying patterns in the data. Examination of the confusion matrix (Figure 14) reveals that the model correctly classifies rating class 3 more reliably than others, while classes 2 and 4 are often misclassified as 3, and classes 0, 1, and 5 exhibit similar tendencies. A noteworthy observation is that misclassifications tend to occur between neighboring classes, whereas classes that are further apart, such as 0 and 5, are rarely confused. This suggests that the model is not producing random predictions, but rather that the proximity and overlap of class distributions present inherent challenges in distinguishing closely spaced ratings.

The ROC curves (Figure 15) reinforce this observation, showing relatively low AUC values of approximately 0.54 for all classes, which indicates limited separability among the rating bins. Compared to tasks such as *titleType*, the model struggles to distinguish *rating_bin*, likely due to the continuous and overlapping nature of ratings as opposed to the more discrete and structured categories of title types. Feature importance analysis provides additional insight: *ratingCount* emerges as the strongest predictor, which is intuitive since titles with higher ratings are more likely to be correctly classified. *StartYear* appears influential, potentially reflecting

temporal trends in ratings, while *runtimeMinutes* indicates that longer titles tend to receive higher ratings. Other features such as *totalCredits*, *castNumber*, *totalMedia*, and *tvEpisode* also contribute significantly, with *tvEpisode* being more impactful than other TV formats like *tvMiniseries*, *tvSpecial*, or *tvShort*, possibly due to greater representation in the dataset. Overall, the results suggest that while the model captures broad patterns such as the tendency for longer or more regionally distributed titles to receive higher ratings, it struggles with fine-grained distinctions between closely spaced rating bins.

4.6 Model Comparison

4.7 Explainable AI

To better understand the predictions made by our Neural Network model, we employed LIME Local Interpretable Model-agnostic Explanations to provide local explanations for individual predictions. LIME works by perturbing the input data around a specific instance and observing how the model’s predictions change. This allows us to identify which features are most influential for that particular prediction. For our analysis, we selected the first instance from the test set of both classification tasks: **titleType** and **averageRating**. We then used LIME to generate explanations for the model’s predictions on these instances.

4.7.1 titleType

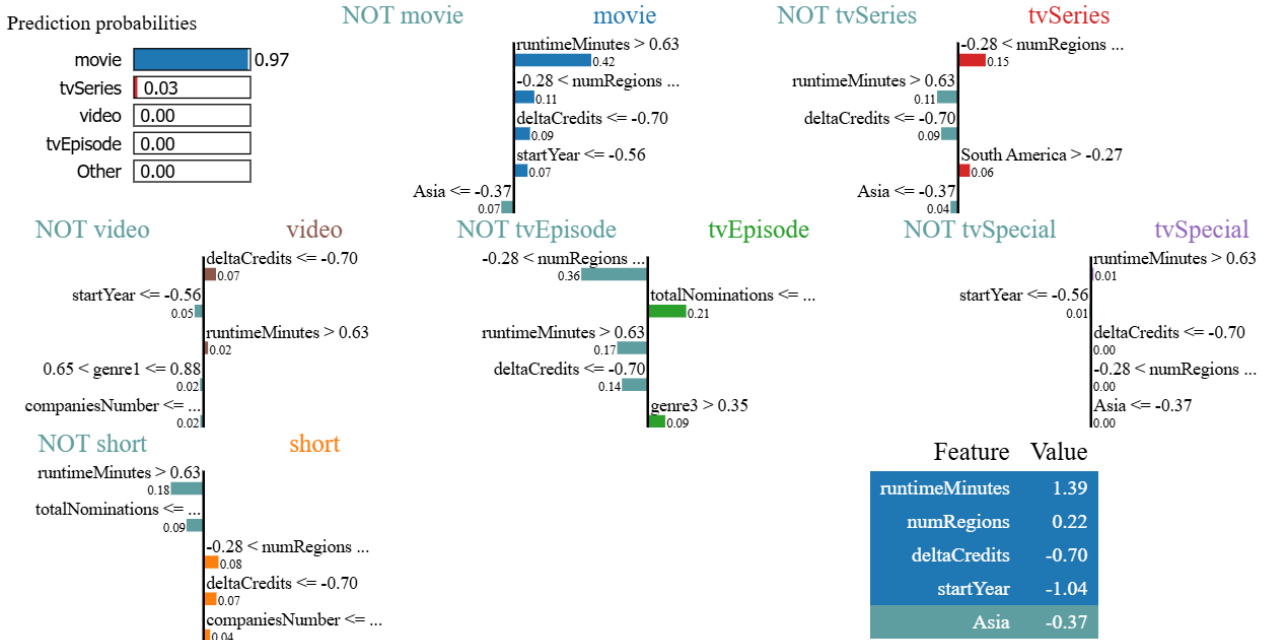


Figure 16: LIME explanation for the **titleType** prediction of instance 0 in the test set.

Figure 16 shows the LIME explanation for the **titleType** prediction of instance 0. We only show the top 5 features for clarity. The model assigns a high probability of 0.97 to the class *movie*, with all other classes receiving negligible scores. This strong confidence is supported by the decision rules extracted from the local surrogate model, which highlight the most influential features contributing to the classification. The top features include *runtimeMinutes*, *numRegions*, *deltaCredits*, and *startYear*, each evaluated against specific thresholds. For instance, the value of *runtimeMinutes* is 1.39 (standardized), which exceeds the threshold used to exclude categories such as *short* and *tvEpisode*, both of which typically have shorter durations. Similarly, the low value of *numRegions* (0.22) and *deltaCredits* (0.01) helps eliminate classes like *video* and *tvSpecial*, which often have limited regional distribution and sparse production metadata. The standardized *startYear* value of -1.04 suggests an older release date, which may align more closely with traditional *movie* formats than episodic or special content. The decision paths shown in the visualization reinforce the model’s reasoning by systematically ruling out alternative classes through feature-based logic. Notably, the absence of branching toward competing categories like *tvSeries* or *video* indicates that the feature profile of this instance is highly aligned with the learned representation of a *movie*.

Figure 17 presents the top five features contributing to the model’s prediction for a specific instance ‘0’ in the **titleType** classification task. The feature *runtimeMinutes* > 0.63 has the highest positive contribution of

Explanation for the top 5 features:

Feature 'runtimeMinutes > 0.63': Contribution: 0.4208
 Feature '-0.28 < numRegions <= 0.57': Contribution: 0.1110
 Feature 'deltaCredits <= -0.70': Contribution: 0.0875
 Feature 'startYear <= -0.56': Contribution: 0.0744
 Feature 'Asia <= -0.37': Contribution: -0.0688

Figure 17: Contribution of top 5 features

0.4208, indicating that longer runtimes strongly support the classification decision, likely favoring categories such as *movie* or *tvSeries*. The condition $-0.28 < \text{numRegions} \leq 0.57$ contributes 0.1110, suggesting that moderate regional distribution adds further support to the predicted class, possibly reflecting titles with limited but non-trivial geographic reach. The feature $\text{deltaCredits} \leq -0.70$, with a contribution of 0.0875, implies that a low difference between director and writer credits may signal a more streamlined or unified production, which is often characteristic of traditional movie formats. The condition $\text{startYear} \leq -0.56$ contributes 0.0744, indicating that older titles are more likely to belong to certain categories, perhaps due to historical production norms or metadata completeness. Interestingly, the feature $\text{Asia} \leq -0.37$ has a negative contribution of -0.0688 , suggesting that limited association with the Asian region reduces the likelihood of certain title types, possibly reflecting regional content trends or distribution biases. Collectively, these contributions reveal how the model leverages both structural and geographic metadata to make confident predictions, and they underscore the interpretability of the decision-making process through localized feature analysis.

4.7.2 averageRating

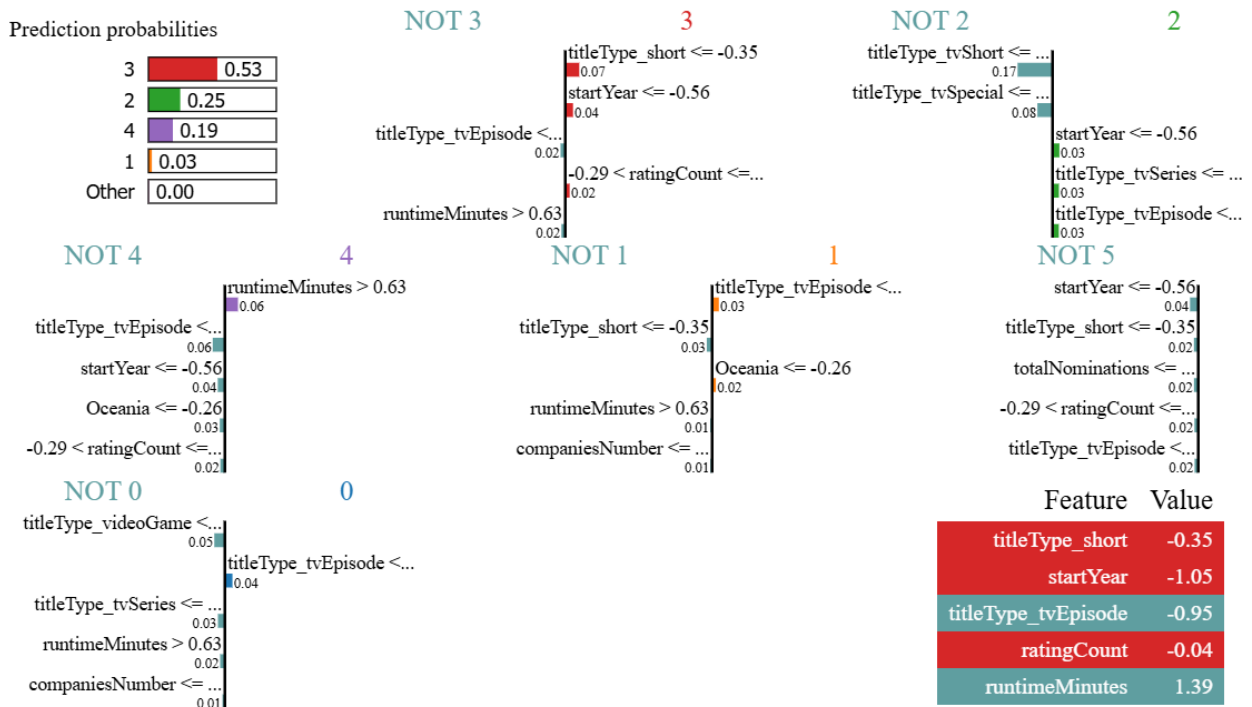


Figure 18: LIME explanation for the `rating_class` prediction of instance 0 in the test set.

Figure 18 presents the LIME explanation for the `rating_class` prediction of instance 0 in the test set, generated from a sequential neural network model. The predicted class is 0, with a confidence of 53%, followed by class 1 (25%), class 2 (13%), and class 3 (9%), indicating a moderate level of uncertainty but a clear preference toward the lowest rating bin. For this instance, $\text{titleType_short} = 0.43$ and $\text{titleType_tvEpisode} = 0.5$ suggest the content is neither a short nor a TV episode, which may steer the model away from mid-range rating bins typically associated with episodic or short-form content. The value $\text{startYear} = -1.05$ indicates an older release, which often correlates with lower ratings due to outdated production standards or limited

Explanation for the top 5 features:

```
Feature 'titleType_short <= -0.35': Contribution: 0.0692
Feature 'startYear <= -0.56': Contribution: 0.0384
Feature 'titleType_tvEpisode <= -0.95': Contribution: -0.0236
Feature '-0.29 < ratingCount <= 0.50': Contribution: 0.0215
Feature 'runtimeMinutes > 0.63': Contribution: -0.0192
```

Figure 19: Contribution of top 5 features

contemporary relevance. Additionally, `ratingCount` = -0.25 reflects low audience engagement, reinforcing the likelihood of a lower rating bin. Interestingly, `runtimeMinutes` = 1.39 suggests a longer duration, which might typically support higher ratings, but in this context, it appears insufficient to offset the negative influence of other features. The surrogate explanation reveals how the neural network integrates temporal, structural, and popularity-related metadata to arrive at its prediction, and it highlights the nuanced interplay between feature thresholds and class probabilities in a locally interpretable manner.

Figure 19 illustrates the top five features influencing the model’s prediction for the `rating_bin` classification. The feature `titleType_short` ≤ -0.35 contributes positively with a value of 0.0692, suggesting that titles categorized as "short" are more likely to fall into a specific rating bin, possibly due to their niche appeal or limited exposure. The feature `startYear` ≤ -0.56 adds a contribution of 0.0384, potentially reflecting historical rating standards or audience expectations. Conversely, the feature `titleType_tvEpisode` ≤ -0.95 has a negative contribution of -0.0236, implying that the absence or low presence of TV episodes reduces the likelihood of the predicted rating bin, possibly due to episodic content receiving more polarized ratings. The condition $-0.29 < \text{ratingCount} \leq 0.50$ contributes 0.0215, suggesting that moderate rating counts slightly support the classification, likely reflecting a balance between popularity and niche interest. Lastly, `runtimeMinutes` > 0.63 contributes negatively with -0.0192, indicating that longer runtimes may detract from the predicted rating bin, perhaps due to pacing issues or audience fatigue. The model appears to weigh structural metadata (e.g., title type, runtime) alongside temporal and popularity indicators to infer rating categories. Overall, The model’s interpretability lies in its transparent structure, allowing us to trace how each feature contributes to the final classification. This is particularly valuable for validating predictions and identifying potential biases in the training data.

5 Advanced Regression

The chosen target variable is `averageRating`, which represents the average rating (on a 1–10 scale) assigned by IMDb users to each title. The exploratory data analysis showed that its distribution is approximately normal, with most titles concentrated in the range between 6 and 7.

5.1 Random Forest Regression

We applied the *Random Forest Regression* algorithm on the task. Before training the model, although not strictly necessary for tree-based models, we standardized the numerical features for consistency and transformed the categorical feature `titleType` using *One-Hot Encoding*.

The hyperparameters were optimized using *RandomizedSearchCV* with 5-fold cross-validation, exploring different values for the number of trees (100, **200**, 300, 400, 500), the maximum depth (**None**, 10, 15, 20, 25, 30), the minimum number of samples required for a split (2, **5**, 10, 15) and for a leaf (**1**, 2, 4, 6), and the number of features considered at each split (sqrt, **log2**). The best hyperparameters found are highlighted in bold. The R^2 score was used as the evaluation metric during cross-validation.

The optimized Random Forest was first evaluated on the test set (results reported in Table 16). Subsequently, the model was retrained using only the 18 most important features identified through feature importance analysis. Feature selection was guided by a cumulative importance plot, which showed that these 18 features accounted for over 90% of the total importance, effectively reducing the dimensionality from the original 28 features without a significant loss in predictive performance.

Table 16: Performance of the Random Forest Regressor on the test set (full model vs reduced features).

Model	MAE	MSE	R^2
Random Forest (All Features)	0.7536	1.0833	0.4033
Random Forest (Top 18 Features)	0.7550	1.0922	0.3984

The results, reported in Table 16, indicate that the Random Forest model achieves a mean absolute error below one point on the IMDb scale and explains around 40% of the variance in the target variable. Notably, the model trained on only the top 18 features performs almost identically to the full-feature model (R^2 : 0.3984 vs 0.4033), showing that predictive power is concentrated in a limited subset of variables. Feature importance analysis further highlighted that the most influential predictors include both numerical variables, such as `runtimeMinutes`, `startYear`, `ratingCount`, and `deltacredits`, and categorical variables derived from the encoding step, such as `titleType_tvEpisode`, among others.

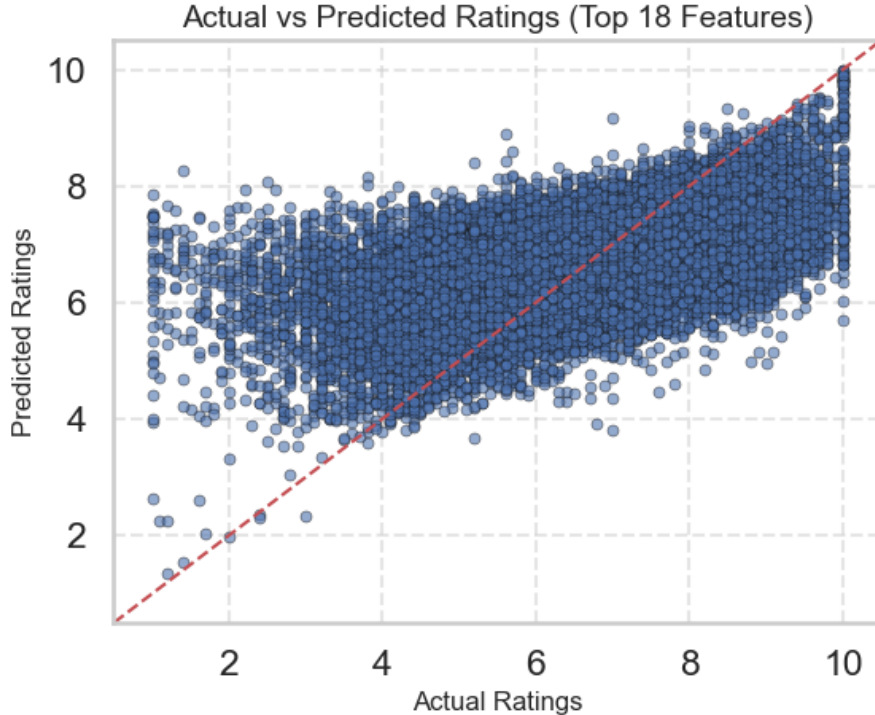


Figure 20: Actual vs Predicted `averageRating` for the Random Forest model trained on the top 18 features.

The scatter plot in Figure 20 shows that the predicted ratings roughly follow the trend of the actual ratings. Most predictions fall in the 6–7 range, consistent with the distribution of the target variable. While the model captures the general pattern, deviations occur, particularly at the extremes, which is consistent with the moderate R^2 of around 0.40. This indicates that the model explains a substantial portion of the variance, but there remains considerable unexplained variability.

5.2 Neural Network Regression

A feedforward neural network was also implemented for the regression task. Table 17 summarizes the performance of the neural network on the test set.

MAE	MSE	R^2
0.7463	1.0791	0.4067

Table 17: Performance of the Neural Network Regressor on the test set.

6 Time Series Analysis

6.1 Data Understanding

The dataset consists of 1134 films, each represented by a time series of daily domestic box-office gross revenues in the United States and Canada, spanning 100 days from release day (day 0) to day 99. Each observation also includes descriptive metadata. The dataset contains 104 attributes in total: 100 numerical columns corresponding to daily gross revenues, one numerical column for the IMDb average `rating`, and three categorical columns identifying the film `id`, `genre`, and `rating category`.

Preliminary inspection revealed no missing values. For films with runs shorter than 100 days, missing entries were completed through a synthetic extension procedure, which imputes values using a noise-augmented mean of the observed revenues. This ensures uniform series length, although it introduces artificial values that may influence analyses focusing on the later days of a film’s lifecycle.

Descriptive statistics provide an overview of the box-office revenue trends. On release day, the average revenue is approximately 9 million USD, with maximum values exceeding 150 million USD. Revenues decline rapidly in subsequent days, reaching mean values near 100000 USD by day 99. Variance remains high across the series, indicating substantial variability in revenue levels among films. IMDb ratings show a mean of 6.6 with a standard deviation of 0.9, ranging from 2.8 to 8.7. The **rating_category** variable, which will serve as the target for the classification part, is distributed across five classes:

- **Low** (10 titles), representing ratings ranging from 1.0 to 4.0;
- **Medium Low** (128 titles), representing ratings ranging from 4.1 to 5.5;
- **Medium** (387 titles), representing ratings ranging from 5.6 to 6.5;
- **Medium High** (232 titles), representing ratings from 6.6 to 7.0;
- **High** (377 titles), representing ratings from 7.1 to 10.0.

The distribution is highly imbalanced, with the Low category being significantly underrepresented compared to the other classes.

The presence of extreme values and synthetic extensions may necessitate normalization to ensure comparability of the time series and support more robust analyses.

6.2 Motifs and Anomalies Discovery

6.3 Clustering

6.4 Classification

The classification task aims to predict the **rating_category** of a film based on its daily box-office revenue time series. This category originally had five classes: Low, Medium Low, Medium, Medium High, and High. However, due to the significant class imbalance, with the Low category containing only 10 instances, the decision was made to merge the Low and Medium Low categories into a single class.

6.4.1 Recurrent Neural Network

As the last model, a Recurrent Neural Network (RNN) was implemented, because of the suitability of RNNs for sequential data. Its architecture is shown in Figure 21.

The architecture was obtained through experimentation with different configurations and hyperparameters. The test and validation sets used 40% of the dataset each, while the training set used the remaining 60%. The split was stratified, to maintain class proportions across sets.

The genre features are handled the same way as in previous Neural Networks (a Dense layer with 8 neurons and ReLU activation function, the right-most branch in figure 21).

The time series data is processed through an encoder-decoder architecture, to extract relevant features from the sequences. The encoder processes the first half of the time series, with two Bidirectional LSTM layers (with 32 and 64 units respectively). The decoder processes the second half of the time series, with two Bidirectional LSTM layers (with 64 and 32 units respectively). The final shape resembles a diamond shape, with the number of units first increasing, then decreasing, to capture both local and global patterns in the data. Both the encoder and decoder use recurrent dropout of 0.3 in every layer for regularization.

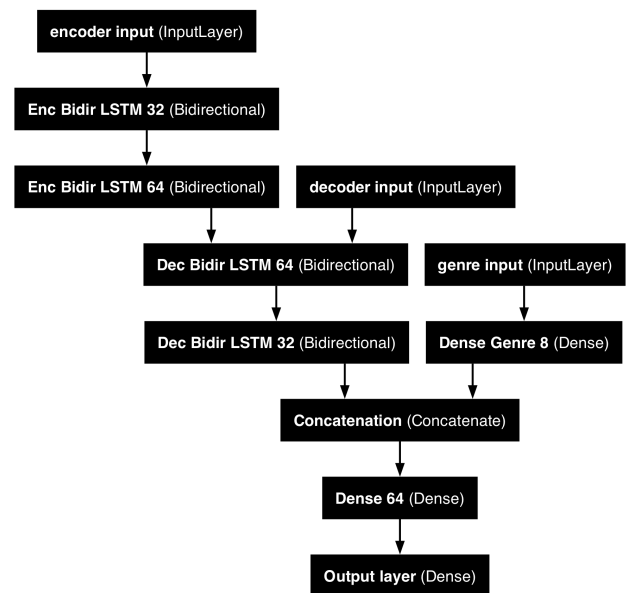


Figure 21: Architecture of the RNN model

The outputs of the two branches are finally concatenated, and fed to a Dense layer with 64 neurons and ReLU activation function, followed by a Dropout layer with rate 0.3. The final output layer has 4 neurons (one for each class) and a Softmax activation function. Wherever possible, Batch Normalization was applied to speed up training and improve stability.

The model was trained using the Adam optimizer, categorical cross-entropy loss function and a learning rate of 0.005. Early stopping was employed to halt training if the validation loss did not improve for 20 consecutive epochs. The model was trained for a maximum of 200 epochs with a batch size of 32, considering balanced class weights.

Figure 22 shows the evolution of training and validation loss and accuracy over epochs.

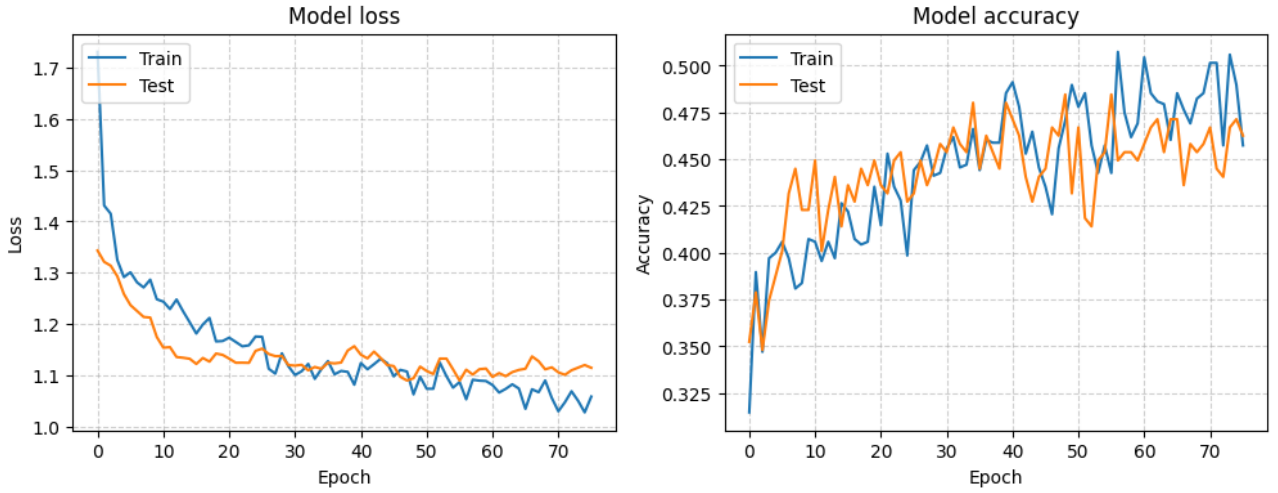


Figure 22: Training and validation loss and accuracy over epochs

The loss curves show incremental improvement over epochs, with relative stability. Their shape do not indicate overfitting, as the validation loss seems to find relative stability around the 50th epoch. Accuracy curves seem to confirm that overfitting is not a central issue. They also show significant instability, likely due to the small size of the dataset, which makes the small sizes of validation and test sets more susceptible to changes in the model's behavior.

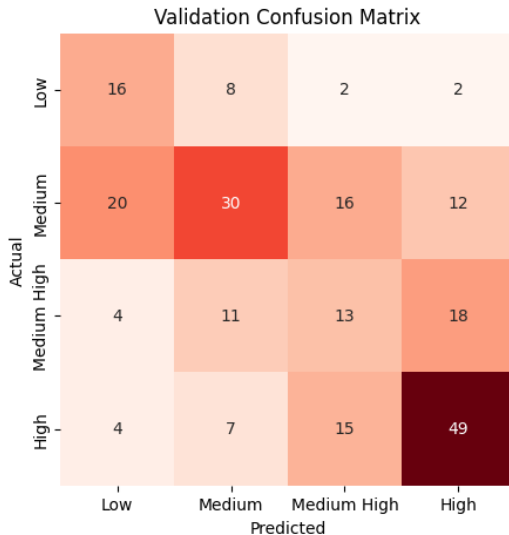


Figure 23 shows the confusion matrix for the RNN model on the test set.

Both **Low** and **Medium High** classes struggle a bit, likely because of their small size. Likely because of balanced class weights, both of them often get confused with adjacent classes.

The **Medium** class seems to be generally hard to distinguish. It also represents the only frequent case of non-adjacent class misclassification, as its instances are often misclassified as **High**. This overall difficulty could be due to high overlap between this class and the others.

Figure 23: Confusion matrix for the RNN model on the test set

Table 18 shows the macro and weighted average precision, recall, and F1-score for the RNN model. The final model's accuracy represents a relatively satisfactory result, especially considering the small size of the dataset and class imbalance. Both macro and weighted averages can also be considered decent, indicating that the model performs reasonably well across all classes, without being overly biased towards the more frequent ones.

Metric	Precision	Recall	F1-score
Macro avg	0.45	0.47	0.45
Weighted avg	0.49	0.48	0.47
Accuracy			0.48

Table 18: Macro and weighted average precision, recall, and F1-score for the RNN model